Surface Science 90 (1979) 676–687

INVESTIGATION OF OXYGEN ADSORPTION ON Cu(110) BY LOW-ENERGY ION BOMBARDMENT

A.G.J. DE WIT, R.P.N. BRONCKERS, Th.M. HUPKENS and J.M. FLUIT
Fysisch Laboratorium Rijksuniversiteit Utrecht, Princetonplein 5, Utrecht, The Netherlands

Received 24 November 1978; manuscript received in final form 6 February 1979

The interaction of molecular oxygen with a Cu(110) surface is investigated by means of low energy ion scattering (LEIS) and secondary ion emission. The position of chemisorbed oxygen relative to the matrix atoms of the Cu(110) surface could be determined using a shadow cone model, from measurements of Ne^+ ions scattered by adsorbed oxygen atoms. The adsorbed oxygen atoms are situated 0.6 ± 0.1 Å below the midpoint between two adjacent atoms in a ⟨100⟩ surface row. The results of the measurements of the ion impact desorption of adsorbed oxygen suggest a dominating contribution of sputtering processes. Ion focussing effects also contributes to the oxygen desorption. The ion induced and the spontaneous oxygen adsorption processes are studied using different experimental methods. Sticking probability values obtained during ion bombardment show a strong increase due to the ion bombardment.

1. Introduction

The interaction of molecular oxygen with copper single crystal surfaces of various orientations has been the subject of investigations since the advent of ultra high vacuum techniques. The subjects of interest are the adsorption and desorption of molecular as well as atomic oxygen on the surface and also the arrangement of the adsorbate and of the substrate due to oxygen exposure of the surface.

The adsorption of oxygen on Cu(110) at pressures between 10^{-8} and 10^{-4} Torr has been investigated with Low Energy Electron Diffraction (LEED) [1–4] and work function measurements [5]. Recently the kinetics of oxygen interaction with a Cu(110) surface have also been studied with Auger Electron Spectroscopy (AES) and ellipsometry [6]. The results of these investigations suggest that at room temperature the initial sticking coefficient (S_0) for a clean crystal surface is about 10^{-1} and that the adsorption process can be described with a model in which dissociative chemisorption of oxygen is assumed. The LEED patterns initially show streaks parallel to the ⟨110⟩ directions, changing into a (2 × 1) structure after an exposure of (6–60) × 10^{-5} Torr sec. Further exposure at room temperature causes an increase in background intensity and the appearance of weak spots of a c(6 × 2) structure [1,2].

Some phenomena relating to adsorbed oxygen on single crystal surfaces have also been investigated with Low Energy Ion Scattering (LEIS). For example the oxygen position on a Ag(110) surface was determined by Heiland et al. [7]. The oxygen position on a Cu(110) surface was investigated with LEIS by De Wit et al. The results have been discussed extensively in a previous paper [8].

Studies on the sputtering of adsorbates by low energy ions showed that the stimulated desorption of adsorbed species depends on the ion energy, the ion–adsorbate–substrate combinations, the position of the adsorbed atoms relative to the matrix atoms and the binding energies of the adsorbed species [9–12]. In this paper experimental results concerning desorption and adsorption processes will be presented for the Cu(110) surface. It will be shown that the stimulated desorption process can be studied properly when the oxygen position is known. The results of the measurements concerning the adsorption during ion bombardment can be interpreted when the stimulated desorption cross section is known.

2. Theoretical introduction to the formation of an adsorbed layer.

In this part of the paper the formation of an adsorbed layer and the consequences of the formation of this layer on the sticking of the adsorbed species will be discussed briefly. Although a wide variety of events [13,14] are possible when a diatomic molecule is incident on a metal single crystal surface with twofold symmetry, only a few assumptions concerning the formation of an adsorbed layer are needed for the experimental methods we used. These assumptions are as follows:

(1) The incident molecule has a certain probability of becoming dissociatively chemisorbed on the surface. This sticking probability depends on the coverage of the surface by chemisorbed oxygen atoms (θ_1).

(2) The residence time of the chemisorbed atoms is very long compared to the time scale of the experiments.

(3) The coverage by the physisorbed molecules (θ_2) is very slight, so hardly any contribution is to be expected from these molecules in signals related to the chemisorbed oxygen atoms.

It can be shown that the above mentioned assumptions are justified for the oxygen–copper system at room temperature [6,15]. In the case of ion bombardment on an oxygen exposed metal surface the increase of the chemisorbed oxygen coverage in a time interval dt can now be written as

$$\mathrm{d}\theta_1 = S(\theta_1)(v/\theta_m)\,\mathrm{d}t - \sigma I_0 \theta_1\,\mathrm{d}t\,, \tag{1}$$

where v is the number of incident oxygen molecules per cm^2 surface area per sec, $S(\theta_1)$ is the probability that an incident oxygen molecule will become dissociatively chemisorbed (sticking probability), θ_m is the number of maximum available chemisorption sites per cm^2, I_0 is the number of incident ions per cm^2 surface area per sec and σ is the cross section for desorption of a chemisorbed oxygen atom by an incident ion (desorption cross section).

The sticking probability $S(\theta_1)$, which depends on the adsorption and desorption rates of the physisorbed molecular oxygen and on the interaction energies between the chemisorbed oxygen atoms, appears to be influenced by the ion bombardment. In the case of ion bombardment the sticking probability will therefore be written as

$$S(\theta_1) = S_1(\theta_1) + S_2(\theta_1)\,, \tag{2}$$

where $S_1(\theta_1)$ is the sticking probability due to spontaneous adsorption processes and $S_2(\theta_1)$ is the sticking probability due to ion induced adsorption processes.

The induced desorption cross sections of chemisorbed oxygen on a Cu(110) surface will be determined and the sticking probabilities with and without ion bombardment will be deduced from the given experimental results by means of relations (1) and (2).

3. Experimental set-up and handling

The experiments were performed by bombarding the target with low energy noble gas ions (Ne^+ and Ar^+). A Nier-type ion source was used (energy 0.1–10 keV, energy spread 1%, angular spread 1°, current 10 nA to 1 μA, spot-size 4 mm^2). The elevation angle of incidence ϕ and the azimuthal angle of incidence ψ could be varied by means of a target manipulator with an accuracy of 1°. A small double flat-plate electrostatic energy analyzer (rotatable in the plane of incidence, energy resolution 3.5%, solid angle of detection 10^{-3} sterad) was used to measure the ions scattered at the scattering angle θ [16].

The background pressure in the apparatus was 10^{-8}–10^{-9} Torr, measured by a Bayerd–Alpert ionization gauge. A quadrupole mass spectrometer (QMM 17-Riber) was used to measure the oxygen pressure at low partial oxygen pressures. The oxygen was admitted to the UHV system from a gas inlet system via a needle valve. The oxygen pressure was fixed by the equilibrium between a continuous flow of oxygen and the pumping speed of a turbomolecular pump.

The experiments were performed on copper single-crystalline targets at room temperature. The targets were disc-shaped crystals, spark-cut to within 2° of the (110) orientation from a pure (99.999%) copper rod obtained from Material Research Corporation. After grinding and electro-lap polishing the crystal it was mounted in the target manipulator. The surface was cleaned by sputtering with 3 keV Ne^+ or Ar^+ ions at a small elevation angle of incidence (20°) (ion dose of about 10^{17} ions/cm^2). After this cleaning procedure hardly any contribution of surface defects or crystal surface imperfections were detectable in the measured ion scattering energy spectra.

Obtained energy spectra show peaks from secondary ions and from scattered ions at about the energy for single scattering by copper and oxygen atoms. These scattering peaks, as well as the low energy contribution of secondary ions, were used to study the adsorption and desorption from a Cu surface.

4. The oxygen position at the Cu(110) surface

Fig. 1 shows some of the results for 3 keV Ne^+ ions scattered by oxygen atoms in the Cu(110) surface over a scattering angle of 45°. The peaks in these azimuthal distributions can be interpreted as an enlarged flux of Ne^+ ions scattered by oxygen atoms which are located at the edge of the shadow cone formed by copper atoms in the first surface layer [8]. At $\phi = 9°$ and $\psi = 35°$ the separation of the peaks I and II is at its maximum. From this fact and from the symmetry of the azimuthal distributions it follows that the centre of the adsorbed oxygen atom on the Cu(110) surface lies 0.6 ± 0.1 Å below the midpoint between two neighbouring Cu atoms in a ⟨001⟩ row.

The position of the oxygen is used to calculate the ϕ and ψ values for which the oxygen lies at the edge of the shadow cone of other Cu surface atoms. The results

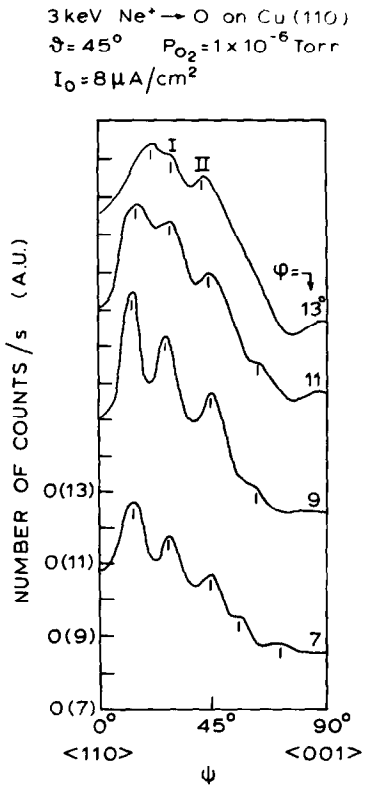

Fig. 1 Measured yields of Ne^+ ions scattered by O atoms chemisorbed on a Cu(110) surface as a function of the azimuthal angle ψ for the various angles of incidence φ indicated. The curves are separated by a vertical shift of the origin (0(7), 0(9),...).

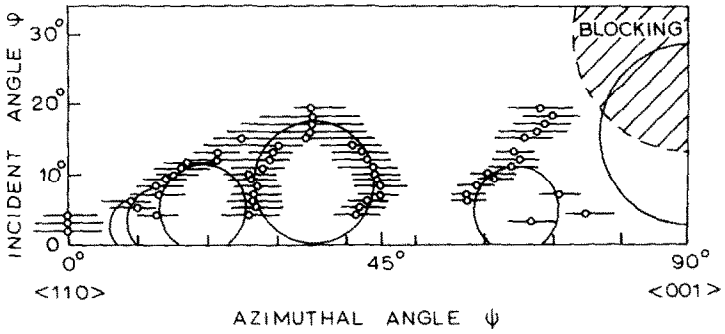

Fig. 2. A $\varphi-\psi$ diagram of the peak positions as deduced from curves shown in fig. 1. (○) peak position with bar indicating the peak width. The circles represent the shadow cones calculated for different copper lattice atoms in the neighbourhood of an adsorbed O atom situated 0.6 Å below the midpoint between two adjacent Cu atoms in an ⟨001⟩ surface row.

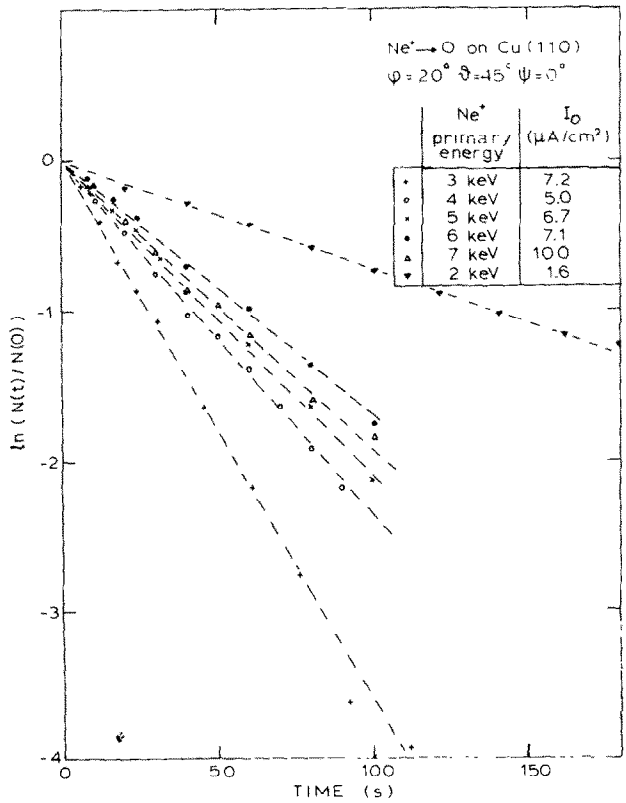

Fig. 3. Decrease of the normalized scattering yield from an oxygen exposed (1000 L) Cu(110) surface due to Ne^+ ion bombardment, plotted as a function of the bombarding time.

of these calculations (using an inverse square power potential) are the circles in the $\phi-\psi$ diagram (fig. 2). Distortion of the shadow cone by neighbouring atoms has not been taken into account. Peak positions deduced from several azimuthal distributions are given in fig. 2 together with bars which indicate the peak widths. An extensive discussion of the results is given in ref. [8]. From fig. 2 it can be concluded that the directions of incidence used in the desorption measurements described below are such that oxygen atoms are not shadowed by Cu surface atoms. Therefore direct collisions between noble gas ions and oxygen atoms are possible.

5. Determination of the desorption cross section

If the measured ion scattering signal from oxygen is assumed to be proportional to the density of oxygen atoms at the surface, the following equation for the intensity of the signal can be derived from eq. (1)

$$N(t) = CI_0\theta_1(0)\exp(-I_0\sigma t)\,. \tag{3}$$

C contains the scattering cross section and the probability that a particle will leave

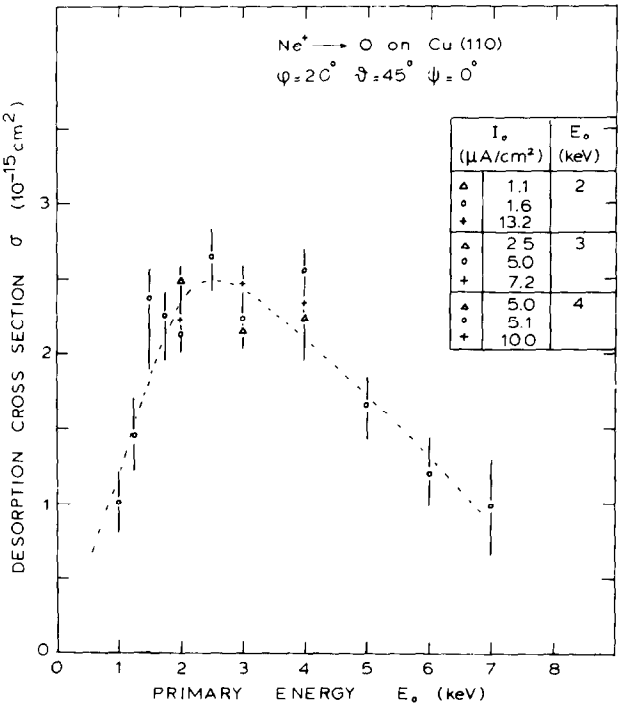

Fig. 4. Cross sections for the desorption of adsorbed O on Cu(110) by Ne^+ ion bombardment as a function of the primary ion energy (ion scattering method).

the surface in the form of an ion. The stimulated desorption cross section σ is determined from the scattering signal as a function of time and the known primary particle current density I_0 [17]. The above approach is possible for the sputtered secondary ions because of a linear increase in the sputter ion yield with increasing oxygen coverage [18]. No background corrections are necessary because of the low sputter ion yield from clean copper surfaces at higher secondary ion energies.

Experiments were performed on a Cu(110) surface with oxygen exposures of 1000 L (10^{-5} Torr for 100 sec). The angular settings of the crystal were such that the oxygen atoms are fully visible, as indicated earlier. In fig. 3 the yield of Ne^+ ions scattered by oxygen is shown as a function of time. From the straight lines in fig. 3 the desorption cross sections can be calculated. The desorption cross sections obtained from these and other measurements are given in fig. 4 as function of the primary ion energy. The average desorption cross section in the 2–4 keV energy range corresponds to a desorption rate of 1 atom/ion at a saturation coverage of half a monolayer.

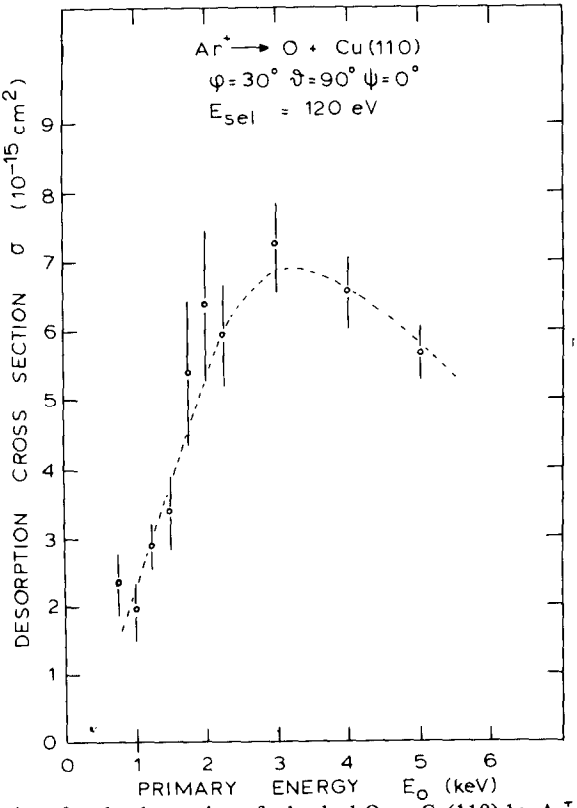

Fig. 5. Cross sections for the desorption of adsorbed O on Cu(110) by Ar^+ ion bombardment as a function of the primary ion energy (secondary ion method).

The desorption cross sections calculated from 120 eV secondary ion emission measurements for Ar^+ ion bombardment are given in fig. 5.

Figs. 4 and 5 show a rather similar shape for the functions $\sigma(E)$. The values of the desorption cross section for Ar^+ ions are a factor 3 higher than for Ne^+ ions.

6. Discussion of the measured desorption cross sections

Three types of mechanism have been proposed which may contribute to the stimulated desorption (Winters and Sigmund [19]). The first mechanism involves direct collisions between the incoming ions and the adsorbed atoms, the second one involves collisions between the adsorbed atoms and primary particles which have been reflected from substrate atoms. The third mechanism involves the collision cascade which has been created by the impinging ion and which results in the desorption of adsorbed species by sputtered substrate material. The first and second mechanisms will cause a decreasing desorption cross section with increasing primary ion energy, since these contributions are directly related to the total collision cross sections. The contribution caused by the third mechanism is expected to be proportional to the sputtering rate. It is known from sputtering data [20,21] that for copper this rate is at its maximum at some keV primary ion energy. This behaviour is also found in our results given in figs. 4 and 5. Because sputtering data for clean Cu(110) surfaces bombarded with the same ions, at the same energies, and at the same angles are not available a comparison with our experiments is not directly possible. Nevertheless an extrapolation of sputtering data for normal incident ions to our conditions shows a fairly good agreement: the estimated sputtering cross sections as a function of energy coincide with the cross sections for desorption. A remarkable difference between the energy dependency for desorption and for sputtering is the decrease of the desorption cross section at primary energies above 3 keV. The decrease in desorption is much more pronounced.

There is, however, one aspect of the first two mechanisms mentioned which has attracted no attention up till now. Ion focussing by the surface layer copper atoms will increase the flux of primary ions on the oxygen atoms below. Preliminary calculations indicate a strongly increased flux of incident particles on the oxygen atom layer at 2–3 keV Ne^+ and 3–4 keV Ar^+ ions. This can explain some of the above-mentioned differences in behaviour. Comparison of our experimental results with the work of Taglauer et al. [9–12] is difficult because of the different adsorbate–substrate combination and the fact that their work gives no data above 2 keV.

7. Experimental study of adsorption and the determination of the sticking coefficient

The sticking coefficients, obtained without direct influence of the ion bombardment, are determined from measurements of ion signals directly after a period of

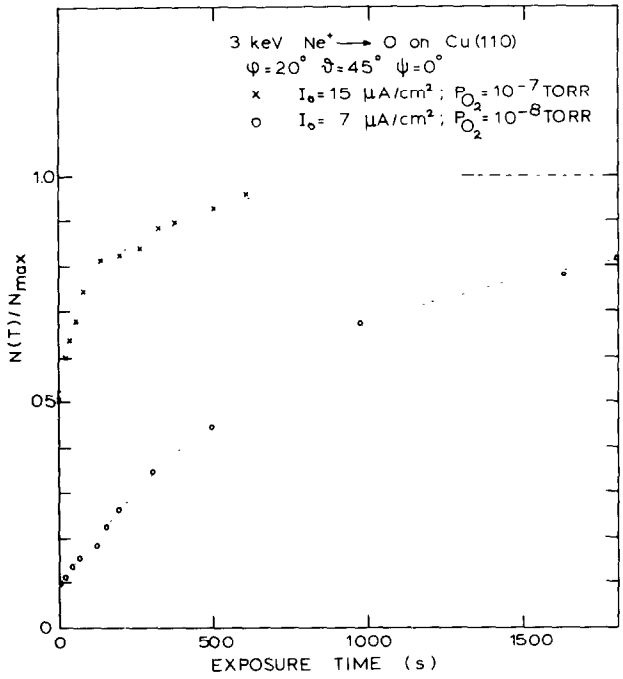

Fig. 6. Normalized number of counts for Ne^+ ions scattered by O as a function of the time that the copper surface is exposed to oxygen with the ion beam off, measured directly after the onset of the Ne^+ ion beam.

time T in which the beam was switched off. The relative yields $N(T)/N_{max}$ for 3 keV Ne^+ ions scattered by oxygen are given in fig. 6. The curve shows the increase of the signal as a function of the exposure time, starting from the dynamic equilibrium between adsorption and desorption at $T = 0$ sec.

The sticking coefficient is calculated from these results with the relation derived from eq. (1):

$$S(\theta_1) = \frac{\theta_m}{v}\frac{d\theta_1}{dT} = \frac{\theta_m}{vN_{max}}\frac{dN(T)}{dT}\theta_{max} . \tag{4}$$

N_{max} is the ion signal at saturation coverage θ_{max}. The results are given in fig. 7. The normalized sticking coefficients $S_n(\theta_1) \equiv S(\theta_1)/\theta_{max}$ are independent of the assumed value of θ_{max}. In our case $\theta_{max} = 0.25$ molecule/site can be substituted [6]. The extrapolated value of $S(0)$ is 0.10 ± 0.01 (for $\theta_{max} = 0.25$), which agrees with the results of Habraken et al. [6].

The sticking coefficient during Ar^+ ion bombardment was determined from measurements performed after the dynamical equilibrium between adsorption and desorption ($d\theta_1/dt = 0$) of oxygen had been reached. The secondary ion emission

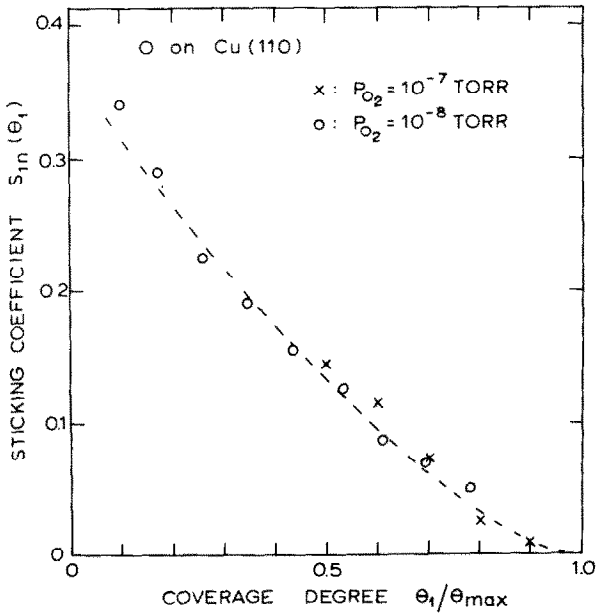

Fig. 7. The sticking coefficient for oxygen impinging on Cu(110) as a function of the oxygen coverage on the surface.

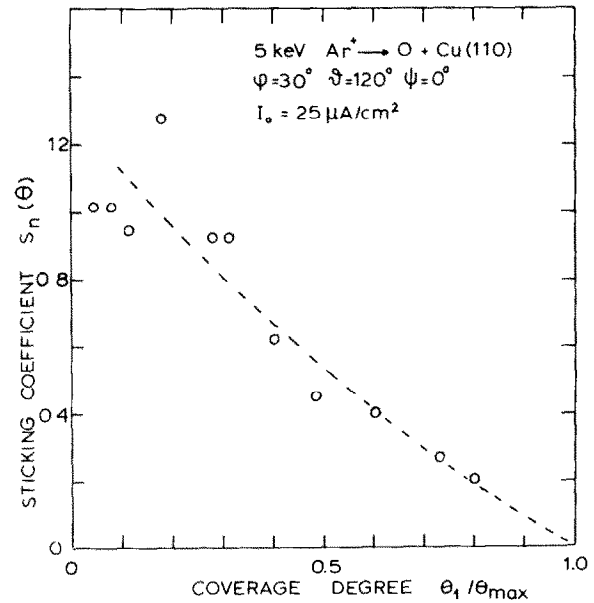

Fig. 8. The sticking coefficient for oxygen impinging on Cu(110) during Ar^+ ion bombardment, plotted as a function of the oxygen coverage.

signal was measured with fixed primary ion intensity at different oxygen pressures. The sticking probability is calculated from

$$S(\theta_1) = S_1(\theta_1) + S_2(\theta_1) = \frac{\theta_m}{\upsilon}\left[\frac{N(\upsilon)}{N_{max}} I_0 \sigma\right] \theta_{max}\,, \tag{5}$$

where $N(\upsilon)/N_{max} = \theta_1/\theta_{max}$ and the value of σ is taken from the experimental results given in section 5. Here, σ is taken to be 6×10^{-15} cm^2 to obtain the results shown in fig. 8 which are for 5 keV Ar^+ ions at an angle of 30°.

8. Discussion of the measured sticking coefficient

The sticking probabilities as well as the shape of the curves obtained from those measurements in which the influence of the ion bombardment is negligible are in reasonable agreement with results given by other authors [6]. The shape of the sticking probability curve of fig. 7 cannot be explained by simple Langmuir kinetics where a $(1 - \theta_1)$ or $(1 - \theta_1)^2$ dependency would be expected. Even when ordering in the adsorbed layer is taken into account in the kinetic model [22], it is hardly possible to explain the observed behaviour of the sticking coefficients. Therefore, we conclude that a kinetic model in which the oxygen adsorbs dissociatively via a mobile precursor state in which a twofold symmetric ordering in the adsorbed layer is useful [15]. Preliminary results of calculations based on this model are promising.

Comparison of the shapes of the sticking probability curves obtained from measurements with and without ion bombardment (fig. 7 and fig. 8) show a remarkable similarity, suggesting a similar kinetic model for both processes.

It can be seen from fig. 3 that if the signal is measured immediately after the ion beam is switched on the measured yield corresponds to the coverage of an unbombarded oxygen-covered surface. Sticking coefficients for a partially oxygen-covered surface during 25 μA/cm^2 Ar^+ bombardment were presented in fig. 8. Preliminary experiments at other ion current densities show a linear behaviour of the sticking coefficients for a given value of θ. Extrapolation to $I_0 = 0$ gives sticking coefficient values which are close to those of fig. 7. This means that $S_2(\theta_1)$ is directly related to the momentary influence of a penetrating ion. We believe that the ion creates a disturbed surface area where oxygen sticking is more likely to occur.

More experimental and theoretical investigations to support the presented description are in progress.

Acknowledgements

This work is part of the research program of the Stichting voor Fundamenteel Onderzoek der Materie (FOM) and was made possible by financial support from the

Nederlandse Organisatie voor Zuiver Wetenschappelijk Onderzoek (ZWO). We thank W.C. Post and G.B. Crielaard for their technical assistance.

References

[1] G. Ertl, Surface Sci. 6 (1967) 208.
[2] G.W. Simmons, D.F. Mitchell and K.R. Lawless, Surface Sci. 8 (1967) 130.
[3] A. Oustry, L. Lafourcade and A. Escaut, Surface Sci. 40 (1973) 545.
[4] N. Takahashi, H. Tomita and S. Motoo, Compt. Rend. (Paris) 269B (1969) 618.
[5] T.A. Delchar, Surface Sci. 27 (1971) 11.
[6] F.H.P.M. Habraken and G.A. Bootsma, Ned. Tijdschr. Vakuum Techn. 16 (1978) 142 (ECOSS I, Amsterdam, 1978)
[7] W. Heiland, F. Iberl and E. Taglauer and S. Menzel, Surface Sci. 53 (1975) 383.
[8] A.G.J. de Wit, R.P.N. Bronckers and J.M. Fluit, Surface Sci. 82 (1979) 177.
[9] E. Taglauer, U. Beitat, G. Marin and W. Heiland, J. Nucl. Mater. 63 (1976) 193.
[10] E. Taglauer, G. Marin and W. Heiland, Appl. Phys. 13 (1977) 47.
[11] E. Taglauer, G. Marin, W. Heiland and U. Beitat, Surface Sci. 63 (1977) 507.
[12] E. Taglauer, U. Beitat and W.Heiland, Nucl. Instr. Methods 149 (1978) 605.
[13] P.A. Redhead, H.P. Hobson and E.V. Kornelsen, The Physical Basis of Ultra-High Vacuum (Chapman and Hall, London, 1968).
[14] F.O. Goodman, Surface Sci. 26 (1971) 327.
[15] A.G.J. de Wit, R.P.N. Bronckers, Th.M. Hupkens and J.M. Fluit, to be published; A.G.J. de Wit, Thesis, Utrecht (1979).
[16] A. van Veen, A.G.J. de Wit, G.A. van der Schootbrugge and J.M. Fluit, J. Phys. E (Sci. Instr.) 12 (1979) 861.
[17] I_0 is the number of incident ions per cm^2 surface area per second. Note, that the desorption cross section σ, as defined in this paper, has to be multiplied by $\sin \varphi$ to obtain the cross section familiar in gas–atom collision theory.
[18] A. Benninghoven, Z. Physik 230 (1970) 403.
[19] H.F. Winters and P. Sigmund, J. Appl. Phys. 45 (1974) 4760.
[20] A.L. Southern, W.R. Willis and M.T. Robinson, J. Appl. Phys. 34 (1963) 153.
[21] G.D. Magnuson and C.E. Carlston, J. Appl. Phys. 34 (1963) 3267; Phys. Rev. 138 (1965) 759.
[22] D.A. King and M.G. Wells, Proc. Roy. Soc. (London) A339 (1974) 245.